Showcasing research from Professor Jun Hee Jang's laboratory, Department of Chemical Engineering, Rowan University, New Jersey, USA.

Facile fractionation of spent coffee grounds into sustainable aviation fuel-relevant streams using methanol and potential endogenous alcohol–glycerol solvent mixtures

Spent coffee grounds, a lipid-containing lignocellulosic waste, are fractionated through an alcohol-based solvolysis strategy into streams enriched in lipids, lignin, and carbohydrates. This integrated approach leverages endogenous solvent effects to provide a direct and circular pathway toward sustainable aviation fuel production.

Image reproduced by permission of Jun Hee Jang from *Green Chem.*, 2026, **28**, 6226.

Cover artwork created using Google Gemini.

As featured in:

See Jun Hee Jang *et al.*, *Green Chem.*, 2026, **28**, 6226.

ROYAL SOCIETY OF CHEMISTRY

rsc.li/greenchem

Registered charity number: 207890

Green Chemistry

PAPER

View Article Online
View Journal | View Issue

Cite this: *Green Chem.*, 2026, **28**, 6226

Facile fractionation of spent coffee grounds into sustainable aviation fuel-relevant streams using methanol and potential endogenous alcohol–glycerol solvent mixtures

Christopher Acquah,[a] Kerby C. Jones,[b] Victor T. Wyatt,[b] Valerie García-Negrón,[b] Emmanuel A. Aboagye,[c] Wo Bin Bae,[a] Ishmaiah E. Small,[a] Jack E. Kleissler,[a] Joseph F. Stanzione, III[a,d] and Jun Hee Jang *[a,d]

Spent coffee grounds (SCG), an abundant lignocellulosic biomass waste, offer potential for sustainable aviation fuels (SAF) production due to their major components of carbohydrates (50%), lignin (30%), and lipids (8%), with efficient fractionation being the main challenge. This study presents an alcohol-based solvolysis strategy for deconstructing SCG into SAF-relevant fractions while enabling the use of ethanol and glycerol as endogenous co-solvents. Methanol solvolysis achieved high retentions of glucan (99.5% at 180 °C and 98.0% at 200 °C), mannan (99.0% at 180 °C and 79.0% at 200 °C), and galactan (93.0% at 180 °C and 78.0% at 200 °C), with delipidification (>95.0%) and delignification (>52.0%). The ethanol/glycerol (1 : 1 v/v) co-solvent at 200 °C demonstrated comparable glucan and mannan retentions of 88.0% and 76.0%, with delignification (67.0%) and delipidification (93.0%). All tested solvent systems yielded a combined 61–66 wt% of SAF-convertible lipid, lignin, and carbohydrate fractions, each suitable for direct integration into established catalytic upgrading pathways. Despite the comparable fractionation efficiency, the endogenous solvent systems reduced autogenous pressure to 15.6 bar, 59% lower than neat methanol solvolysis, enabling safer, more energy-efficient biorefinery operation. Techno-economic analysis shows superior performance for co-solvent systems, with ethanol/glycerol achieving a minimum selling price (MSP) of $1.43 per kg and methanol/glycerol achieving $1.64 per kg, which are 30% and 20% lower than methanol solvolysis ($2.05 per kg) while delivering enhanced solvent circularity and operational safety.

Received 16th December 2025,
Accepted 5th March 2026

DOI: 10.1039/d5gc06813d

rsc.li/greenchem

Green foundation

1. This work advances green chemistry by introducing an integrated solvolysis-based fractionation of spent coffee grounds using endogenous alcohol–glycerol solvent systems. By valorizing all major biomass components into relevant streams, the process enhances resource efficiency, promotes solvent circularity, and reduces reliance on external hazardous solvents.
2. The process achieves simultaneous recovery of lipid-, lignin-, and carbohydrate-derived SAF substrates with a combined yield of 61–66 wt% based on spent coffee grounds. Using endogenous solvents reduces autogenous pressure by 59% compared to conventional methanol solvolysis, improving process safety and lowering the minimum selling price by up to 30%.
3. Future work will focus on moisture-tolerant operation to reduce drying energy, catalytic upgrading of mixed product streams, and broader life-cycle and green-metric evaluation.

Introduction

Sustainable aviation fuels (SAF) have emerged as a biobased alternative allowing airlines to diversify their fuel supplies. SAF are chemically similar to conventional jet fuels and can be seamlessly integrated into existing aircraft engines without modification, positioning them as the most viable short- to mid-term pathway to aviation decarbonization.[1,2] The United States, through its SAF Grand Challenge, targets the production of approximately 9.1 million tonnes (Mt) of SAF

[a]*Department of Chemical Engineering, Rowan University, Glassboro, NJ 08028, USA. E-mail: jang@rowan.edu*
[b]*Sustainable Biofuels and Co-Products Research Unit, Eastern Regional Research Center, USDA-ARS, Wyndmoor, PA 19038, USA*
[c]*Department of Chemical and Biological Engineering, Princeton University, Princeton, NJ 08544, USA*
[d]*Advanced Materials & Manufacturing Institute (AMMI), Rowan University, 201 Mullica Hill Road, Glassboro, New Jersey 08028, USA*

annually by 2030 and approximately 106 Mt by 2050, supported by strong policy incentives.[3–5] The European Union, through its ReFuelEU Aviation Initiative, mandates a minimum 6% SAF blend in aviation fuel by 2030, increasing progressively to 70% by 2050.[5–7] These initiatives create a strong demand for the increased use of SAF. Despite this strong policy momentum, actual production remains far behind targets, with global SAF production at only 1.0 Mt in 2024 and projected to grow to just 2.1 Mt in 2025.[8,9]

The current landscape of SAF primarily revolves around commercially mature technologies such as hydroprocessed esters and fatty acids (HEFA) and the increasingly adopted alcohol-to-jet (ATJ) pathways.[10–12] HEFA, converting lipids from feedstocks such as vegetable oils, waste fats, and used cooking oil into C8–C16 jet-range hydrocarbons through catalytic hydrotreating and isomerization, dominates today's SAF market.[13,14] Major producers operating commercial-scale HEFA-based SAF production facilities include Neste, World Energy, TotalEnergies, and Eni.[15,16] Ethanol-to-jet (ETJ) converts bioethanol, produced from saccharification and fermentation of carbohydrates, into jet-range hydrocarbons *via* catalytic carbon–carbon coupling.[17–19] While HEFA and ETJ are promising for producing linear and branched alkanes, hydrodeoxygenation (HDO) of lignin-derived monomers and dimers has recently attracted significant attention as an emerging pathway for producing aromatics and cycloalkanes, which account for 4–25% of aviation fuel.[20–22]

Despite advances in SAF technologies, feedstock supply remains a critical bottleneck in scaling SAF production, primarily due to challenges related to both feedstock availability and accessibility.[23–27] Availability constraints reflect limited sustainable quantities of biomass, particularly lipid and (hemi)cellulose-based feedstocks. These feedstocks face intense competition from other biofuel sectors and, even under optimistic scenarios, are projected to meet less than 10% of global jet fuel demand by 2050.[27–29] Lignocellulosic biomass, though theoretically abundant, is significantly constrained by factors such as seasonal harvesting, competing uses (soil carbon retention, animal feed, and bioenergy), and challenging supply chain logistics, collectively reducing the actual quantity feasible for SAF production.[29–31] Moreover, lignocellulose is increasingly routed to other higher-value fuels, chemicals, and materials. These include carbohydrate-derived platform molecules (*e.g.*, furfural, 5-hydroxymethylfurfural, and their downstream monomers, xylitol, and organic acids such as lactic and succinic acid), lignin-derived aromatics and building blocks (*e.g.*, BTX-range aromatics and 2-pyrone-4,6-dicarboxylic acid), and cellulose and lignin-based materials (*e.g.*, cellulose nanofibrils, resins/foams, polyurethanes/adhesives, and carbon fibers).[32–39] Additionally, feedstock accessibility presents significant technical hurdles in efficiently extracting valuable components, including lipids and fermentable sugars from recalcitrant biomass.[31,40]

Given these feedstock limitations, spent coffee grounds (SCG) represent a promising, underutilized biomass feedstock providing three key advantages for SAF production.[41,42] SCG are an abundantly available biomass resource, generated globally in substantial quantities of approximately 6 Mt annually as waste from coffee brewing.[43,44] SCG are non-food waste materials and have significantly lower procurement costs compared to other biomass feedstocks.[45] SCG exhibit a biochemical composition highly suitable for the established SAF conversion pathways, containing approximately 50–60% carbohydrates, 8–20% lipids, and 20–30% lignin, corresponding to ATJ, HEFA, and HDO processes, respectively.[46–50] Despite this promise, efficient fractionation and extraction of SCG components remain significant technical challenges that require further innovation and development to fully realize SCG's potential in commercial-scale SAF applications.[51–53]

Previous studies on SCG valorization have focused on extracting only certain components, particularly lipids and (hemi)cellulose, and converting them into biofuels, without establishing a comprehensive fractionation strategy.[54–59] Conventional fractionation methods, including acid treatment, steam explosion, and enzymatic hydrolysis, often result in incomplete biomass separation and structural degradation, yielding limited recovery of targeted fractions.[60–62] Solvent-based fractionation (solvolysis) offers a promising approach for lignocellulosic biomass by enabling the one-pot separation of major components.[63–67] In alcohol-based solvolysis of lipid-containing biomass, lipids are extracted into the alcohol phase and can be converted to fatty acid esters with glycerol as a byproduct.[68] Recently, alcohol-solvolysis strategies have been widely applied in lignin-first biorefining to fractionate lignocellulosic biomass and enhance lignin solubilization.[69] However, prior solvent-based SCG studies, while demonstrating valuable progress (Table S1), vary widely in emphasis and scope: many primarily target oil or extractive recovery, whereas others employ sequential unit operations to access specific components such as carbohydrates or lignin.[55,70–73]

This study applies alcohol-based solvolysis to SCG to solubilize lignin and lipids, to catalyze transesterification of the extracted lipids, and to retain (hemi)cellulose in the solid residue. This fractionation scheme combined with subsequent extraction steps enables efficient fractionation of all SAF-relevant components (lipids, carbohydrates, and lignin). Each recovered stream provides suitable substrates for established catalytic upgrading processes (HEFA, ETJ, and HDO) to produce jet-range hydrocarbons.

In addition, this study explores the circulation of glycerol and ethanol as endogenous co-solvents to minimize the use of exogenous alcohol solvents and to reduce the reaction pressure dictated by solvent volatility.[74–77] Glycerol is generated during lipid transesterification in the solvolytic fractionation step, while ethanol is produced from the carbohydrate stream.[78–80] Both glycerol and ethanol have previously been investigated as alternative solvents for biomass solvolytic fractionation.[80–83] Although glycerol is more expensive than methanol or ethanol on a commodity basis, the integrated concept treats glycerol as an internally generated and recycled co-product rather than an externally purchased solvent. Its incorporation contributes to moderated reaction pressure and improved lignin

solubilization,[84–87] enhancing overall fractionation performance at the system level. Here, methanol alone, methanol/glycerol mixtures, and ethanol/glycerol mixtures are evaluated for fractionation efficiency, and a techno-economic analysis (TEA) to elucidate the economic benefits derived from enhanced solvent circularity and reduced reaction pressure. Alcohol–glycerol solvent mixtures were experimentally tested using commercially sourced solvents to benchmark fractionation performance under controlled conditions. The endogenous solvent configuration was subsequently assessed at the process level based on measured yields, mass balances, and TEA. The ability to efficiently isolate all major biomass fractions through methanol solvolysis and recycled endogenous solvents, combined with SCG's high global availability and favorable biochemical composition, highlights this integrated fractionation approach as a particularly compelling and sustainable pathway for scalable SAF production from SCG.

Experimental section

Materials and biomass preparation

Coffee grounds from a commercially available brand (Lacas Coffee Co., Original City Roast) were uniformly brewed using a KRUPS single-serve drip coffee maker with a reusable filter basket (50 g coffee to 750 mL water) to ensure consistent biomass preparation. The resulting SCG were oven-dried at 105 °C for 24 h and stored in sealed containers at room temperature until use.

Solvolysis reaction

Solvolysis fractionation experiments utilized a Parr Series 5000 multi-reactor system, comprising stainless-steel batch reactors (75 mL capacity) with magnetic agitation, thermocouples, and pressure transducers. Reactors were charged with 3 g dried SCG and 45 mL solvent. Methanol (≥99.8%, ACS grade, Sigma-Aldrich) served as the base-case solvent. For co-solvent systems, methanol/glycerol and ethanol/glycerol mixtures (1 : 1 v/v) were tested, with 22.5 mL of each solvent used to maintain a total volume of 45 mL. Reactors were sealed, purged thrice with nitrogen, pressurized to 1 bar with nitrogen, and heated at controlled temperatures (180 °C, 200 °C, and 220 °C) for 3 h after a 30 min heating ramp. The stirring rate at 900 rpm ensured homogeneity and effective biomass-solvent interaction. With pure methanol, autogenous pressure was approximately 24.2, 38.0, and 55.1 bar at 180, 200, and 220 °C, respectively, while the ethanol/glycerol (1 : 1 v/v) co-solvent system exhibited the lowest pressure at 15.6 bar, followed by the methanol/glycerol (1 : 1 v/v) system at 19.1 bar. After reaction completion, reactors were rapidly cooled to ambient temperature and depressurized.

Post-reaction product separation and characterization

Carbohydrate-rich solid residue. The solid fraction was recovered from the reaction mixture by vacuum filtration, thoroughly washed with 120 mL of fresh methanol or ethanol, depending on the solvent used in the reaction, and subsequently dried at 105 °C until a constant weight was reached. The methanol washing solution was combined with the filtrate from the reaction mixture, and the mixture was collected and stored for further analysis. The lipid content of the washed and dried solid residue was determined using a hexane Soxhlet extraction performed at 160 °C for 5 h. Additionally, the carbohydrate and lignin contents of the solid were quantified following standard NREL two-stage acid hydrolysis protocol as described in the Analytical methods section below.[88]

Solvolysis oil. The combined reaction filtrate and methanol wash were subjected to rotary evaporation to remove the solvent, yielding a concentrated solvolysis oil. This oil was sequentially extracted first with hexane and then with water using equal volumes of 45 mL each. The extraction processes separated the solvolysis oil into three distinct fractions (Fig. 1A): (1) a hexane-soluble phase containing lipids (hereafter referred to hexane-extracted oil), (2) an aqueous-soluble phase, and (3) an undissolved lignin-rich oil. Hexane was removed using rotary evaporation to isolate the hexane-extracted oil. The aqueous phase was dried to remove residual water, and the remaining solids were collected and weighed for subsequent mass balance calculations.

Hexane-extracted oil. The hexane-extracted oil was subjected to comprehensive characterization. Analytical techniques included Fourier transform infrared spectroscopy (FT-IR, Thermo Scientific Nicolet iS50), high-performance liquid chromatography (HPLC; Agilent 1100 series with an evaporative light-scattering detector), gas chromatography coupled with flame ionization detection and mass spectrometry (GC-FID/MS; Agilent 7890B/5977), and nuclear magnetic resonance spectroscopy (NMR; Bruker AVANCE III 400 MHz). For NMR, ^{1}H, ^{13}C, and 2D Heteronuclear Single Quantum Correlation (HSQC) spectra were acquired. Additionally, gel permeation chromatography (GPC; Waters ACQUITY APC system, XT 450 Å 2.5 μm, XT 125 Å 2.5 μm, XT 45 Å 1.7 μm columns, tetrahydrofuran (THF) as the mobile phase) was employed to determine the molecular weight distribution of the oil. For GC-FID quantification, 1,3,5-tri-*tert*-butylbenzene (TTB, ≥98.5%, Ambeed) was used as an internal standard; calibration and sample-preparation details are provided in the SI. General FT-IR, HPLC, NMR, and GC-FID procedures are provided in the SI.

Undissolved lignin-rich oil. The undissolved phase, the residue after subsequent hexane and water extractions from the solvolysis oil, corresponding to the lignin-rich fraction, was characterized by GPC to determine its molecular weight distribution. The oil samples were acetylated to enhance solubility prior to GPC analysis. The sample was stirred in a 50 : 50 (v/v) mixture of acetic anhydride and pyridine (1 mL) at 40 °C for 24 h. The reaction was quenched by adding 1 mL methanol, and solvents were removed under a nitrogen stream; this addition/drying cycle was repeated five times. The acetylated oil was dried overnight under vacuum (~0.7 bar, 40 °C), dissolved in THF, passed through a 0.2 μm filter, and then ana-

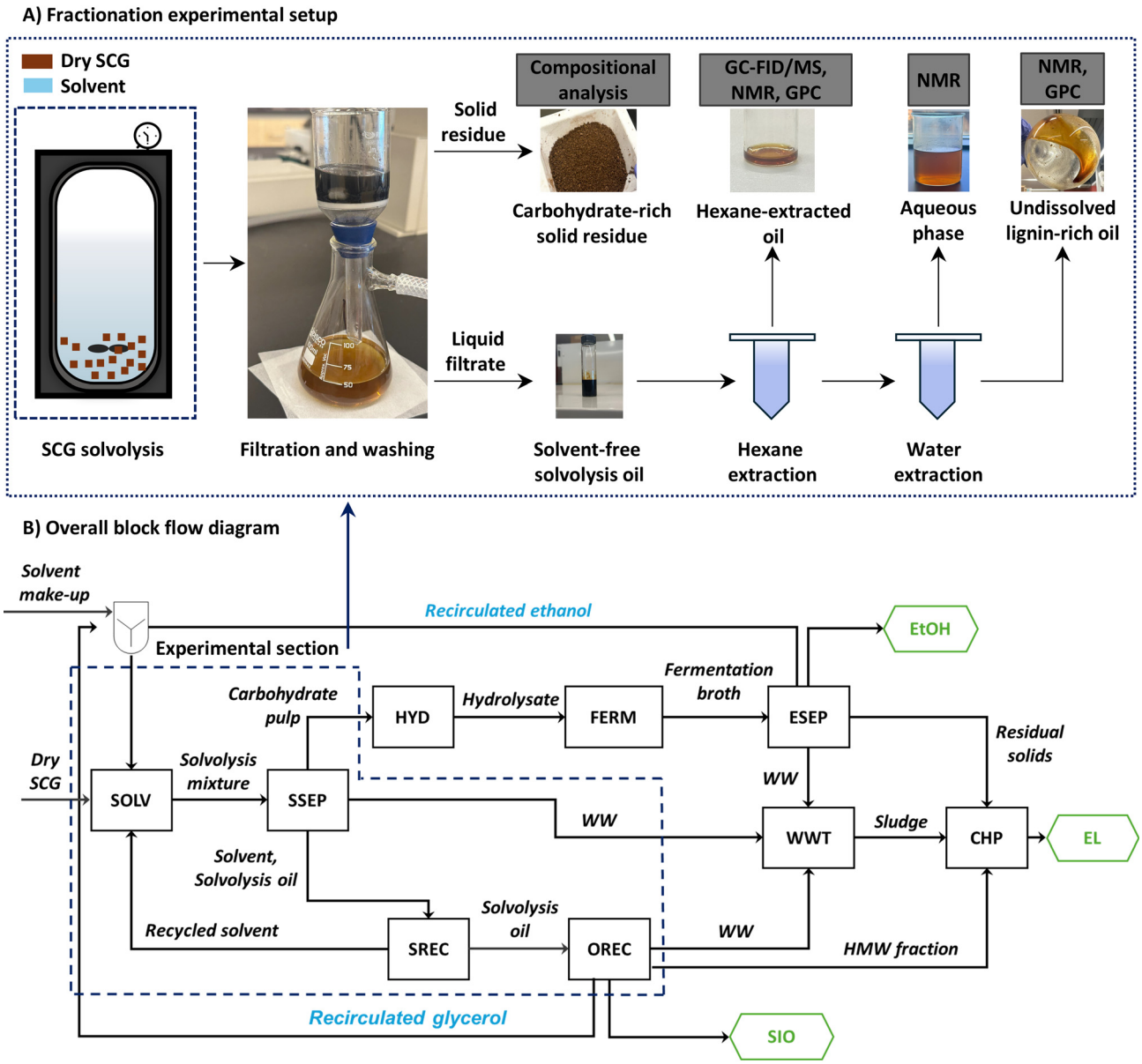

Fig. 1 Integrated SCG solvolysis and biorefinery concept. (A) Experimental alcohol-based fractionation of spent coffee grounds (SCG) into a carbohydrate-rich solid, hexane-extracted oil, water-extracted solubles, and undissolved lignin-rich oil, with associated analytical methods. (B) Process blocks and flows included in the techno-economic analysis (TEA), from SCG solvolysis through solvent recovery with ethanol and glycerol recirculation, hydrolysis/fermentation, and oil recovery to a SAF-intermediate oil and ethanol co-product. The dashed box indicates the experimental section implemented in this study. Abbreviations: SSEP = solvolysis separation; SREC = solvolysis solvent recovery; OREC = SAF-intermediate oil recovery; ESEP = ethanol separation; SOLV = solvolysis; HYD = hydrolysis; FERM = fermentation; WWT = wastewater treatment; CHP = combined heat and power; hexagon = major products (SAF-intermediate oil (SIO)/ethanol (EtOH)/electricity (EL)).

lyzed by GPC. Structural characterization of this undissolved lignin-rich phase was further performed using NMR.

Analytical methods

Compositional analysis. Biomass compositional analysis was conducted using standard National Renewable Energy Laboratory (NREL) protocols.[88] Biomass composition was measured in triplicate following the NREL two-stage acid hydrolysis protocol (report NREL-TP-510-42618) with moisture correction. Acid-insoluble lignin was determined gravimetrically; acid-soluble lignin by ultraviolet-visible spectroscopy (UV-Vis). Hydrolysate sugars were quantified by HPLC (Aminex HPX-87P, 80 °C, water mobile phase, 0.6 mL min^{-1}). Protein was estimated from total nitrogen using a 6.25 conversion factor. Lipids were quantified by hexane Soxhlet extraction and confirmed by accelerated solvent extraction. Further methodological details are provided in the SI.

Thin-layer chromatography. Neutral-lipid class separation used silica gel plates developed in hexane : diethyl ether : acetic acid (80 : 20 : 1, v/v/v). Plates were visualized with 5% phosphomolybdic acid in ethanol and heating. Additional information and detailed protocols are provided in the SI.

HPLC of neutral-lipids. Neutral-lipid classes were quantified by HPLC on a cyanopropyl (CN) column with evaporative light-scattering detector (ELSD) using a hexane and methyl *tert*-butyl ether gradient containing 0.4% acetic acid; calibration followed established neutral-lipid standards. The full gradient and detector parameters are given in the SI.

GC-MS/FID. Hexane-extracted oils were identified by GC-MS (Agilent 8890/5977) using an SP-2380 column (30 m × 0.25 mm × 0.20 μm). The oven temperature was initially held at 50 °C for 1 minute, then increased at 30 °C min^{-1} to 180 °C, followed by a ramp of 2 °C min^{-1} to 210 °C, where it was held for 5 minutes with helium as a carrier gas at 1.0 mL min^{-1}. Injector temperature was 210 °C with a split ratio of 5 : 1, and the transfer line was maintained at 240 °C. For methyl esters quantification, GC-FID (Agilent 7890B) was employed with an HP-5MS column (30 m × 0.25 mm × 0.25 μm). Helium was used as the carrier gas at 0.4588 mL min^{-1} (constant flow). Injector temperature was 280 °C with a split ratio of 100 : 1. The oven program was 70 °C (2 min), ramped at 5 °C min^{-1} to 280 °C (2 min). The FID was maintained at 300 °C with hydrogen at 30 mL min^{-1}, air at 400 mL min^{-1}, and make-up He at 5 mL min^{-1}. The total run time was 46 min. Samples for FID were prepared with 1,3,5-tri-*tert*-butylbenzene (TTB) as an internal standard (20.0 mg oil + 10.0 mg TTB to 1.00 mL MeOH), and mass fractions were calculated by internal-standard ratios with response-factor correction (calibration details in the SI).

Process modelling and techno-economic analysis

An integrated solvolysis-based biorefinery for SCG was developed on an nth-plant basis with a processing capacity of 2000 dry metric tons per day. Aspen Plus v14 was used to model the process. Capital and operating costs were estimated based on equipment sizing together with material and utility requirements, and all values were expressed in 2023 USD. The minimum selling price (MSP) of the SAF-intermediate oil, defined as the combined hexane-extracted oil and the SAF-range fraction of the undissolved lignin-rich oil, was determined using discounted cash-flow analysis at a net present value of zero, assuming a 30-year plant life and a 20% internal rate of return. Ethanol and surplus electricity were included as co-product credits. Further process assumptions and costing details are provided in the SI.

Results and discussion

Fractionation efficiency of methanol-based solvolysis

SCG exhibit a highly favorable composition for multi-pathway SAF production, containing 8.4 wt% glucan, 10.2 wt% galactan, 30.7 wt% mannan, 30.6 wt% lignin including both acid-insoluble and acid-soluble fractions, and 8.0 wt% lipid (Fig. 2A). With about 88.0 wt% of their constituents (lignin, carbohydrates, and lipids) potentially convertible into jet-range hydrocarbons (C8–C16), SCG serve as a promising candidate for integrated biorefining with SAF conversion technologies.

As the base case, methanol-based solvolysis was conducted at 200 °C (MS_200), followed by sequential separation steps, effectively fractionating SCG into distinct product streams: a carbohydrate-rich solid residue, a hexane-extracted oil containing lipids and lower molecular weight lignin fragments, and an undissolved lignin-rich oil (Fig. 2B, see also Fig. 1A). Fractionation efficiency metrics were determined by comparing the compositions of the dried SCG feedstock and the solid residue after solvolysis (Fig. 2C, see also Table S2). In this study, extraction efficiency is used for lignin (delignification) and lipids (delipidification), while retention efficiency is used for carbohydrates. At 200 °C in methanol, SCG exhibited 94.4% delipidification and 52.9% delignification. The high lipid extraction extent is consistent with previously reported *in situ* methanolic transesterification, which typically achieves 90–100% conversion of coffee lipids to fatty acid methyl ester (FAME) in one-pot workflows.[59,89,90] The 52.9% delignification aligns with the 50–70% range commonly reported for alcohol solvolysis from 175 to 235 °C for hardwood biomass.[91,92] Glucan retention was 98.0%, while hemicellulose retention was 78 to 79% for both mannan and galactan (Fig. 2C). These values are consistent with carbohydrate preservation reported in alcohol-assisted fractionation studies on lignocellulosic biomasses, where cellulose retention typically exceeds 90% and hemicellulose retention varies 60 to 90% depending on conditions.[63,91]

To further enhance hemicellulose retention, a lower temperature of 180 °C (MS_180) was tested. This milder condition substantially improved mannan and galactan retention to 99.3% and 92.6%, respectively, while maintaining high glucan retention (99.5%) in the solid phase without sacrificing delipidification (95.7%) or delignification (51.6%). The enhanced hemicellulose retention at reduced temperature occurs because hemicellulose, owing to its amorphous structure and weaker lignin–carbohydrate linkages, is more readily solubilized by alcohol solvents at higher solvolysis temperatures than the more crystalline cellulose fraction.[91,93] A higher temperature of 220 °C was additionally tested to increase lignin extraction extent and facilitate transesterification of the extracted lipids. At 220 °C (MS_220), delignification increased slightly to 57.1%, and delipidification remained at 95.0%. However, hemicellulose retention fell to 62.9% (mannan) and 68.9% (galactan) while glucan remained 96.3%. Because this higher temperature provided only a modest increase in delignification, it represents an unfavorable trade-off for efficient fractionation due to the reduced hemicellulose retention.

For the mass balance analysis (Fig. 2B), masses of each product and intermediate stream were measured (solvolysis oil, solid residue, hexane-extracted oil, water-extracted solids, undissolved lignin-rich oil, as shown in Fig. 1A). After each solvolysis reaction, the combined liquid phase comprising the

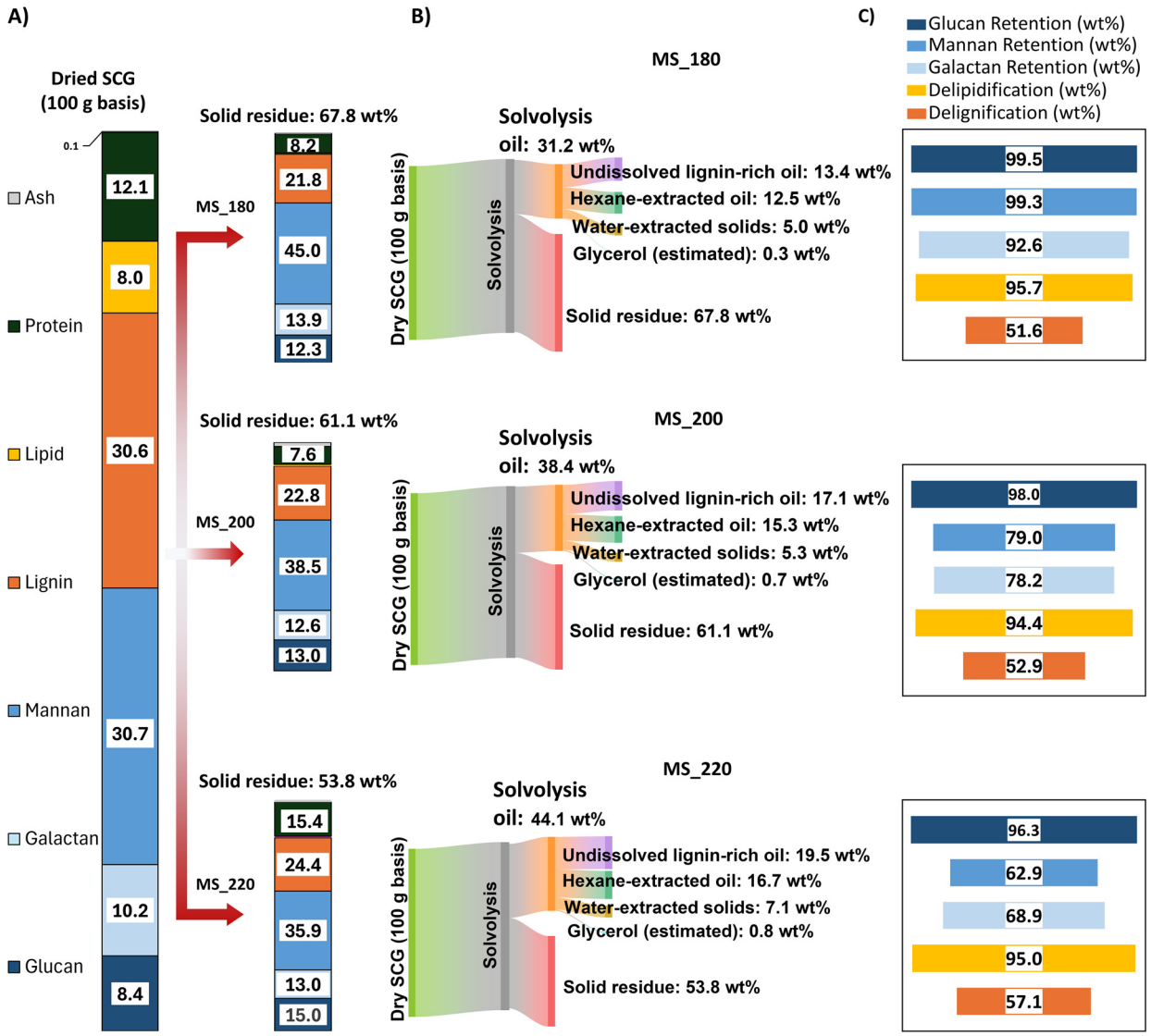

Fig. 2 (A) Compositional profile of dried SCG (per 100 g basis) and solid residue from methanol-based solvolysis at 180 °C (MS_180), 200 °C (MS_200), and 220 °C (MS_220). (B) Overall mass balance per 100 g dried SCG: solvolysis oil yield partitioned into hexane-extracted oil, undissolved lignin-rich oil, water-extracted solids, and glycerol (estimated), plus solid-residue yield; stream yields calculated using eqn (S5)–(S7). (C) Fractionation metrics after methanol solvolysis calculated using eqn (S1)–(S4). Reaction conditions: 3 g dried SCG in 45 mL methanol; T = 180/200/220 °C; 3 h after a 30 min heat-up. Table S2 contains the quantitative information of compositional analysis data shown here. Table S3 contains literature-reported compositional profiles of dried SCG. Table S4 summarizes stream-by-stream characterization and key values.

reaction liquor and the methanol washing filtrate was subjected to rotary evaporation to isolate the solvolysis oil. The solvolysis oil was first extracted with hexane to recover lipid derivatives and low molecular weight, less-polar fragments, followed by water extraction to recover water-extracted solids and glycerol. Glycerol formation from *in situ* transesterification or hydrolysis of SCG-extracted glycerides was observed by ^{1}H NMR of the water extract (Fig. S1). To estimate the amount of glycerol produced, glycerides, FAME, and fatty acids were quantified before and after solvolysis, assuming that removal of the three acyl chains from a triglyceride, whether forming FAME or fatty acids, produces one glycerol.

Mass balances were calculated on a dry basis by summing the constant-weight masses of the four product streams (solid residue, hexane-extracted oil, undissolved lignin-rich oil, and water-extracted solids), with glycerol reported separately as "glycerol (estimated)" and included in the solvolysis-oil total. The overall mass balances on a 100 g dried-SCG basis total 99.0 wt% (MS_180), 99.5 wt% (MS_200), and 97.9 wt% (MS_220). In MS_180, the solvolysis oil is 31.2 wt%, partitioned into 12.5 wt% hexane-extracted oil, 13.4 wt% undissolved lignin-rich oil, 5.0 wt% water-extracted solids, and an estimated 0.3 wt% glycerol, leaving 67.8 wt% as solid residue. In MS_200, the solvolysis oil increases to 38.4 wt% (15.3 wt%

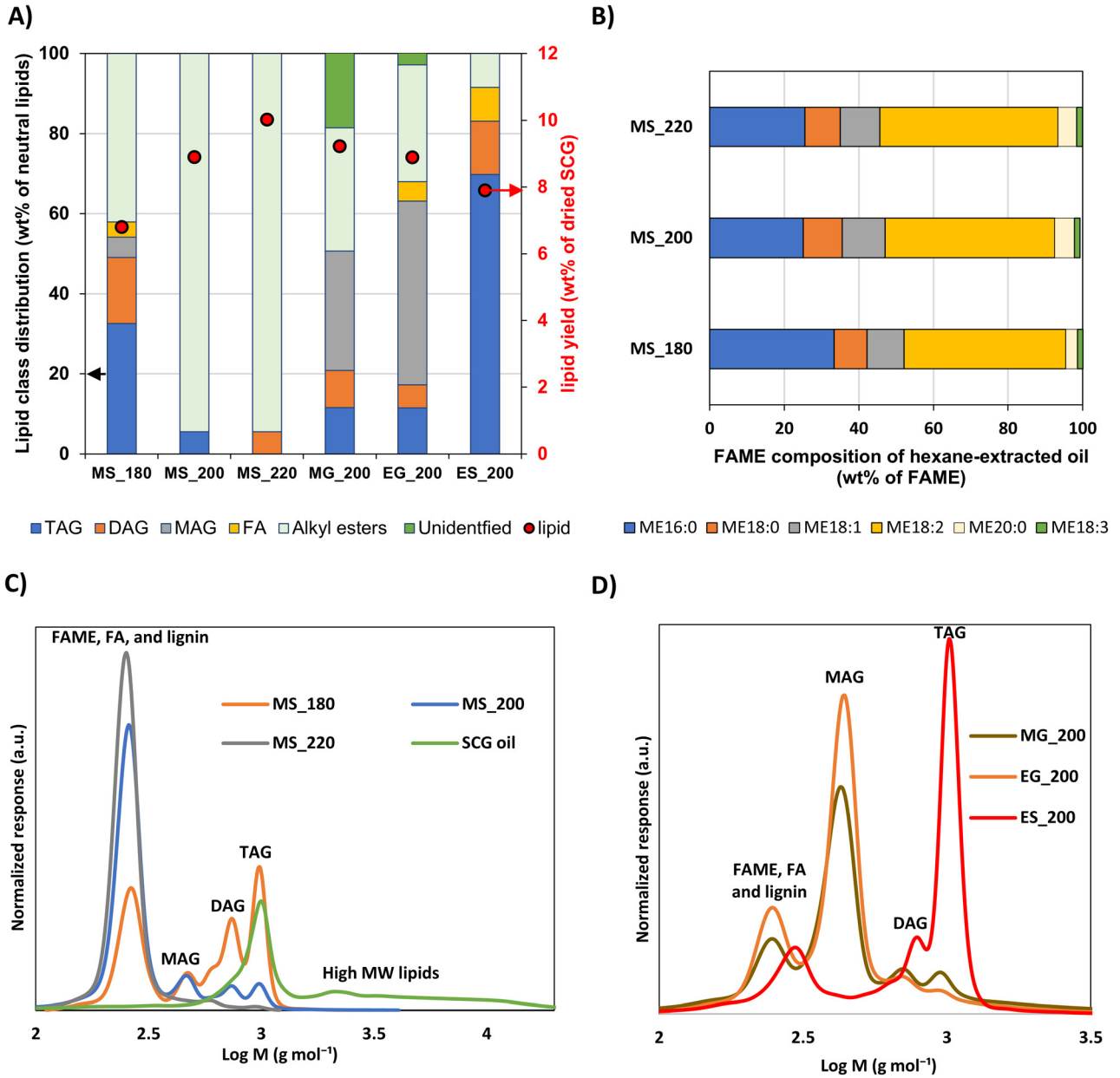

Fig. 3 Hexane-extracted oil characterization. (A) Neutral-lipid class distribution (wt% of neutral-lipids) for MS_180, MS_200, MS_220, ES_200 (ethanol solvolysis at 200 °C), MG_200 (methanol/glycerol solvolysis at 200 °C), and EG_200 (ethanol/glycerol solvolysis at 200 °C) analyzed by HPLC. Alkyl ester species were quantified by GC-FID, and total neutral lipid yields were estimated by back-calculating from the GC-FID-determined alkyl ester mass and their fractional contribution within the neutral lipid classes determined by HPLC. (B) FAME composition of hexane-extracted oil (wt% of FAME) analyzed by GC-MS. (C and D) GPC traces. "SCG oil" is the direct SCG hexane extract. MAG = monoacylglycerols; DAG = diacylglycerols; TAG = triacylglycerols; FA = fatty acids.

hexane-extracted oil, 17.1 wt% lignin-rich oil, 5.3 wt% water-extracted solids, 0.7 wt% glycerol) with 61.1 wt% solid residue. At MS_220, the total oil yield reaches 44.1 wt%, comprising 16.7 wt% hexane-extracted oil, 19.5 wt% lignin-rich oil, 7.1 wt% water-extracted solids and 0.8 wt% glycerol, while the solid residue declines to 53.8 wt%.

The 12–17 wt% hexane-extracted oil obtained between 180 °C and 220 °C exceeds the feed's native ~8 wt% lipid content. GC-FID and HPLC analyses show that lipid derivatives account for 7–10 wt% on a feed basis (Fig. 3A), indicating that the additional 1–2 wt% likely derives from matrix-bound lipids liberated under solvolysis but not recovered by Soxhlet extraction.[94] Overall, lipids represent about 50–60 wt% of the hexane extract; the remainder consists of co-extracted low molecular weight lignin, consistent with aromatic peaks observed in the NMR spectra (Fig. S2). The temperature-driven increase in solvolysis oil and corresponding decrease in solid residue mirror the compositional trends in Fig. 2C: high glucan retention at

180–200 °C, progressive hemicellulose removal, and a slight rise in delignification by 220 °C, while delipidification remains high across the series.

Hexane-extracted oil characterization

The hexane-extracted oil yield rose from 12.5 wt% (MS_180) to 15.3 wt% (MS_200) and 16.7 wt% (MS_220) of dried SCG as solvolysis temperature increased (Fig. 2B). For the methanol cases, increasing solvolysis temperature shifts the extracted lipids toward an ester dominated profile from mixtures of tri-, di-, and mono-glycerides (TAG, DAG, and MAG, respectively). This shift is shown by GPC traces of the hexane-extracted oil (Fig. 3C). The SCG oil, hexane-extracted from dried SCG, exhibited peaks corresponding to TAG (984 Da) and higher molecular weight species up to 4000 Da, which underwent significant reductions in molecular weight through solvolysis, consistent with the HPLC results (Fig. 3A). Notably, solvolysis at 220 °C produced narrowly distributed low molecular weight products including FAME, whereas lower solvolysis temperatures produced a mixture of glycerides, methyl esters, and fatty acids. Higher temperatures help reduce product variability, which may justify sacrificing some hemicellulose extraction for applications requiring high purity FAME. Regardless of the amount of FAME produced from the tested temperatures, methyl palmitate (ME16:0, 270.5 Da) and methyl linoleate (ME18:2, 294.5 Da) are major FAME products as identified and quantified by GC-MS (Fig. 3B). The ^{1}H NMR spectra and FT-IR of the hexane-extracted oil (Fig. S2 and S3) further support these major FAME products.

Lignin-rich oil characterization

Lignin-rich oil was isolated through subsequent hexane-water extractions of solvolysis oil. As the solvolysis temperature increased from 180 to 220 °C, undissolved lignin-rich oil yield rose from 13.4 wt% (MS_180) to 17.1 wt% (MS_200) and 19.5 wt% (MS_220). ^{1}H and HSQC NMR spectra of the lignin-rich oil show characteristic S, G, and H aromatic units together with prominent methoxyl and aliphatic side-chain correlations, indicating a lignin structure enriched in these features (Fig. S4). GPC analysis was conducted after acetylating the oil to improve solubility, as the untreated lignin-rich oil did not fully dissolve in THF. GPC traces revealed a dominant peak at 270–300 Da across all solvolysis temperatures, corresponding to low molecular weight species in the monomer–dimer range that are commonly targeted as lignin-derived intermediates relevant to downstream hydrodeoxygenation (Fig. S5). The lignin-rich oil also contains high molecular weight lignin oligomers and polymers up to 16 000 Da. The SAF-convertible fraction, defined here as species between 110 and 450 Da, accounted for 47–52 wt% of the undissolved lignin-rich oil.

Furthermore, GC-FID analysis of the undissolved oil revealed minor unidentified peaks that may correspond to lignin-derived species. These peaks appeared at longer retention times than those of commonly detected lignin monomers, whereas lignin dimers are generally undetectable without derivatization in GC-FID (Fig. S6). Collectively, these structural and molecular weight analyses indicate that the undissolved lignin-rich oil consists of a heterogeneous mixture of S/G/H units with abundant methoxylated side chains, encompassing both high molecular weight oligomers/polymers and a substantial fraction of low molecular weight species in the monomer–dimer range representing SAF-relevant intermediates for downstream upgrading.

Fractionation efficiency of endogenous solvent cases

Building on the promising performance of methanol in SCG solvolysis, ethanol and glycerol were evaluated as internally generated solvents to improve circularity and reduce reliance on external alcohols. In the proposed scheme (Fig. 1B), ethanol is produced from fermentation of the carbohydrate-rich solid residue, while glycerol is generated *in situ* during catalyst-free lipid transesterification and recovered from the aqueous phase. During the workup process, glycerol partitions into the water-extracted fraction, confirmed by ^{1}H NMR (Fig. S1), and is accounted for in the overall mass balance (Fig. 2B), supporting the feasibility of aqueous-phase recovery prior to recycle. Although commercial solvents were used here for benchmarking, the concept targets fully endogenous operation.

Replacing methanol with ethanol at 200 °C (ES_200) yielded 34.3 wt% solvolysis oil, slightly lower than the 38.4 wt% in MS_200. This oil resulted in 11.7 wt% hexane-extracted oil and 22.6 wt% lignin-rich oil, with the solid residue increased to 64.7 wt% (Fig. 4B). Reduced extraction was reflected in lower delignification (47.4% compared to 52.9% in MS_200) and higher hemicellulose retention (84% compared to 79% in MS_200). Despite the small changes in fractionation efficiency, a clear operational benefit when using ethanol was the lower autogenous pressure of 26.8 bar, compared with 38.0 bar in MS_200 (Fig. S7).

Introducing glycerol as a co-solvent intensified lignin removal while further lowering pressure. Ethanol/glycerol (1 : 1 v/v) at 200 °C (EG_200) produced 43.5 wt% solvolysis oil (15.1 wt% hexane-extracted oil and 26.8 wt% undissolved lignin-rich oil) and 55.2 wt% solid residue (Fig. 4). Delignification reached 67.5%, exceeding MS_200 and ES_200, while delipidification remained high at 92.9%. The trade-off was slightly lower carbohydrate retention, particularly galactan (54.0%), indicating its susceptibility under these conditions. EG_200 operated at the lowest pressure in this study, 15.6 bar at 200 °C. The methanol/glycerol (1 : 1 v/v) blend at 200 °C (MG_200) showed a similar extraction profile to EG_200, with 43.9 wt% solvolysis oil (16.7 wt% hexane-extracted oil and 27.2 wt% undissolved lignin-rich oil) and 54.7 wt% solid residue. Taken together, glycerol co-solvents enhanced lignin solubilization relative to the light alcohols, maintained high delipidification, but increased hemicellulose losses.

Among the conditions tested, EG_200 delivered the highest delignification (67.5%) at the lowest pressure (15.6 bar) while relying entirely on endogenous solvents. Compared to methanol-driven solvolysis (MS_200), the use of ethanol and glycerol as sole solvents or co-solvents inhibited *in situ* transesterifica-

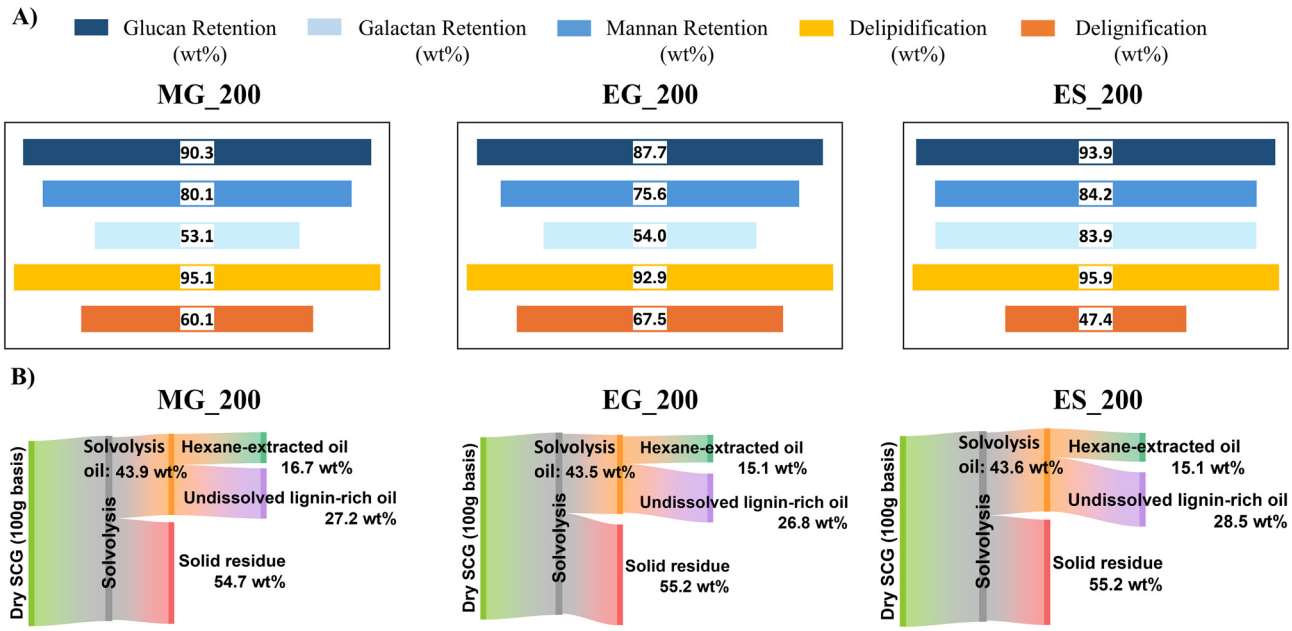

Fig. 4 Endogenous-solvent solvolysis performance. (A) Fractionation metrics for the three recycling cases including methanol/glycerol (MG_200), ethanol/glycerol (EG_200), and ethanol (ES_200). (B) Overall mass balances per 100 g dried SCG for the same three systems, partitioning solvolysis oil into hexane-extractable and undissolved fractions and reporting solid residue yields. Reaction conditions: 3 g dried SCG in 45 mL solvent; MG_200 = methanol/glycerol (1 : 1 v/v), EG_200 = ethanol/glycerol (1 : 1 v/v), ES_200 = ethanol; 200 °C; 3 h after a 30 min heat-up. Table S4 summarizes stream-by-stream characterization and key values.

tion (Fig. 3A). ES_200 produced a TAG-rich hexane-extracted oil with a minor fraction of FAME. When glycerol was used as a co-solvent, the TAG content decreased significantly, and the resulting hexane-extracted oil showed partial transesterification, containing DAG, MAG, and FAME. In summary, introducing glycerol and/or replacing methanol with ethanol reduced operating pressure, slightly altered fractionation efficiency, and moderated the extent of *in situ* transesterification, yielding a broader mixture of lipid-derived products (glycerides and fatty acids) rather than the predominantly FAME profile obtained under neat methanol.

Techno-economic analysis of SCG-to-SAF intermediate biorefinery

An integrated solvolysis-based biorefinery was developed for converting SCG to SAF intermediates, defined as the combined hexane-extracted oil and SAF-range fraction of the undissolved lignin-rich oil, using the experimental data (economic details provided in the SI). Economic analysis reveals substantial advantages for endogenous solvent systems (Fig. 5A). The MSPs are \$2.05 per kg (MS_200), \$1.64 per kg (MG_200), and \$1.43 per kg (EG_200), representing 20% and 30% cost reductions for the co-solvent systems. For the MS_200 case, capital expenditure constitutes the dominant share of the MSP, accounting for 73.7% of the total cost. Within this, the solvolysis area (SOLV in Fig. 1B) contributes approximately 32% (\$0.65 per kg), largely due to the scale and cost intensity of the solvolysis reactor operating at high pressure (38.0 bar). The combined heat and power generation (CHP) area represents another major contributor, responsible for roughly 25% of the MSP. Materials expenses also have a substantial impact, contributing 36.6% of the MSP. Significant cost offset is achieved from ethanol and surplus electricity sales which reduce the MSP by 30.7% (\$0.63 per kg).

Comparable cost distributions are observed in the MG_200 and EG_200 cases, where capital expenditure (CAPEX) similarly dominates the MSP (72.6% and 77.6%, respectively). Materials costs remain the second most significant contributor in both configurations, although the overall solvent demand and hence make-up solvent cost is lower than in the MS_200 system, leading to more favorable MSP outcomes. In the MS_200 case, the highest contribution to the CAPEX is due to the solvolysis reactor in the SOLV area (\$0.65 per kg, \$227 million). This high CAPEX is attributed to the high reactor pressure (38.0 bar). With lower autogenous pressures in the MG_200 (approximately 50% reduction) and EG_200 (approximately 59% reduction) cases, the dominant capital costs shift to the CHP areas (\$0.55 per kg for MG_200; \$0.56 per kg for EG_200).

Operating expenses include substantial costs associated with glucose for producing enzymes used in fermenting carbohydrates to ethanol: \$0.13 per kg (\$19.8 million per year) in the MS_200 case, \$0.12 per kg in the MG_200 case, and \$0.11 per kg in the EG_200 case. These costs reflect the decreasing complexity and solvent-related processing requirements as the systems move toward greater endogenous solvent integration.

Solvent requirements play a significant role in overall process economics. In the MS_200 case, the higher fraction of

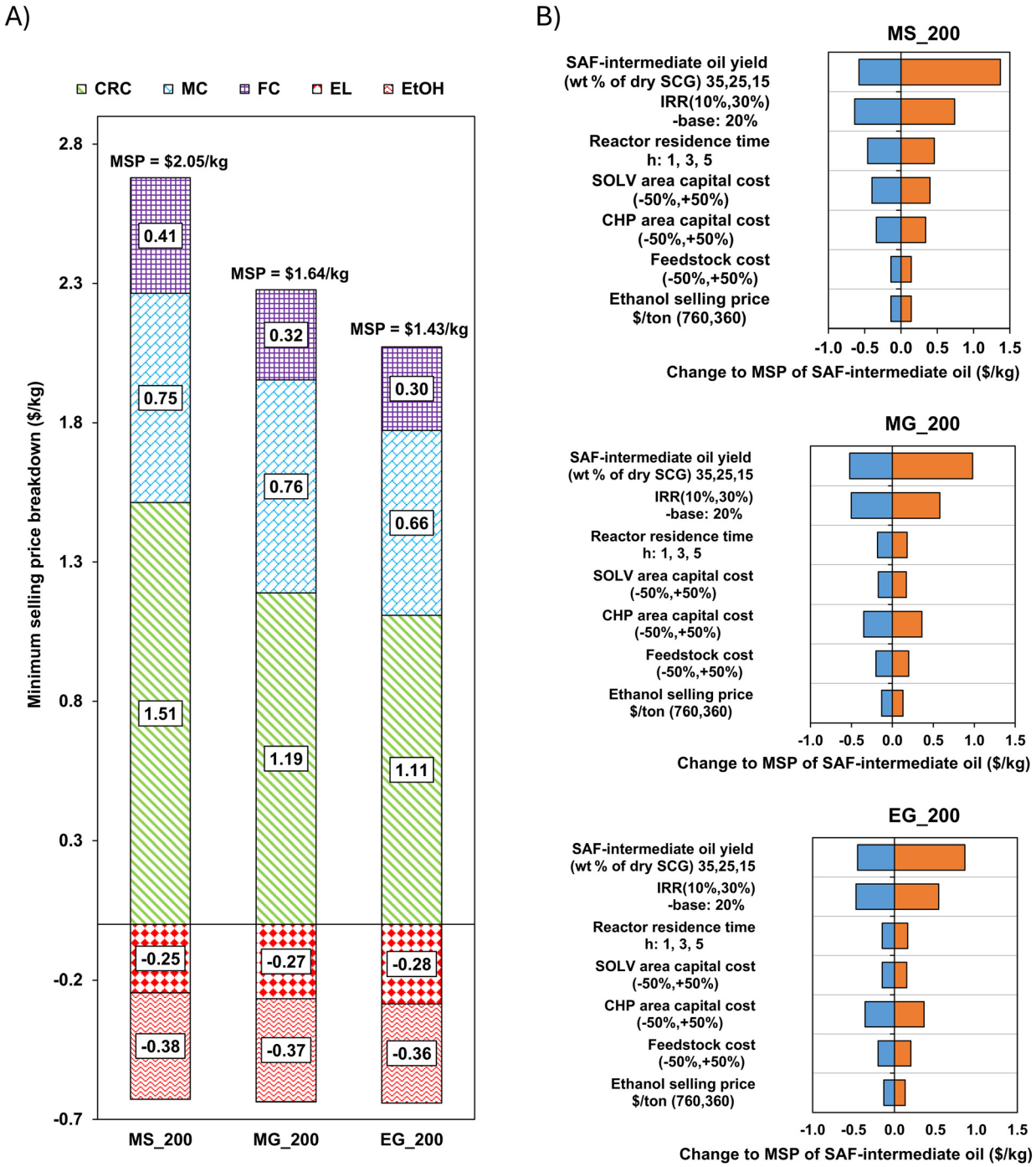

Fig. 5 Techno-economic analysis summary. (A) MSP breakdown ($ per kg) for the SAF-intermediate oil in MS_200, MG_200, and EG_200. CRC, MC, FC are costs; EL and EtOH are credits. CRC = capital recovery charge (capital expenses). MC = material cost (variable operating costs such as feedstock, make-up solvents, glucose for enzymatic hydrolysis, *etc.*). FC = fixed operating cost. EL = revenue from surplus electricity sales. EtOH = revenue from ethanol co-product sale. (B) Single-point sensitivity (tornado) analyses showing change to MSP of SAF-intermediate oil ($ per kg) *versus* oil yield, IRR, residence time, SOLV and CHP area capital costs, feedstock cost, and ethanol price. Abbreviations: SAF, sustainable aviation fuel; MSP, minimum selling price; SOLV, solvolysis area; CHP, combined heat-and-power. Fig. 1B and S8, together with Table S5, provide the integrated process flow diagram and detailed cost breakdown. Fig. S9 presents the sensitivity of MSP to feedstock and drying costs.

alkyl esters (Fig. 3A) leads to increased solvent consumption and correspondingly higher make-up solvent requirements compared to the MG_200 and EG_200 cases. Conversely, the MG_200 and EG_200 systems generate fewer alkyl esters, substantially reducing overall solvent demand. This reduction creates a compounding economic benefit: lower solvent

requirements mean that smaller quantities of endogenous ethanol and glycerol need to be diverted from product streams to serve as make-up solvent for solvolysis. Consequently, the impact on ethanol sales revenue is moderate. In the EG_200 case specifically, although some ethanol is consumed internally, the overall reduction in marketable ethanol is minimal. In the TEA configuration, glycerol is treated as an internally generated and recycled co-solvent; thus, the economic benefit of glycerol-containing systems is reflected primarily in reduced autogenous pressure (and associated capital cost implications) and solvent recovery/separation duties captured in the modeled operating costs, rather than in any assumption of external glycerol purchase.

Single-point sensitivity analysis identifies critical economic parameters affecting biorefinery viability (Fig. 5B). In all three cases, changes in SAF-intermediate oil yields have the highest impacts, followed by the internal rate of return (IRR). The oil yield having the highest impact is expected, since it is the primary product for which the MSP is estimated. Higher yields directly increase the sellable output, thereby improving the revenue base and diluting the impact of fixed and variable costs across a larger product volume (MSP reduction between \$0.5 and \$0.6 per kg). Conversely, lower yields reduce the available product for sale, sharply elevating the MSP (\$0.6 to \$1.4 per kg) because capital and operating expenses must be recovered from a smaller output volume.

An IRR of 20% was used as the base case, with sensitivity bounds evaluated at 10% and 30% to capture the potential impact of varying investor expectations. The base case IRR of 20% reflects the higher risks associated with investments in emerging technologies, including uncertainties in process scale-up, market penetration of co-products, policy support mechanisms, and volatility in biomass supply chains. Increasing the IRR to 30% can significantly increase the MSP by \$0.5 to \$0.7 per kg, thus providing a comparative benchmark while acknowledging the heightened risk premium that would likely be demanded by private investors for first-of-a-kind deployments. Reactor residence time changes have the highest impact in the MS_200 case while moderate impacts are observed for the MG_200 and EG_200 cases, reflecting the pressure-dependent reaction kinetics in the methanol-only system. SCG feedstock cost has a moderate impact on MSP, while variations in ethanol selling price have minimal impact due to the balanced co-product revenue structure.

The integrated analysis establishes that solvent system selection significantly impacts both technical performance and economic outcomes. The EG_200 system emerges as the most economically attractive option, combining favorable reaction pressure with complete solvent self-sufficiency to achieve the lowest MSP while maintaining robust technical performance. This endogenous solvent approach aligns with circular economy principles, enabling solvent self-sufficiency, reducing process severity through lower operating pressures, and improving overall scalability for commercial SAF-intermediate production from SCG feedstock.

Conclusions and remaining challenges

This study establishes alcohol-based solvolysis as an effective approach for fractionating spent coffee grounds (SCG) into sustainable aviation fuels (SAF)-relevant intermediate streams. At 180 and 200 °C, methanol retained up to 99% of glucan, extracted 94–96% of lipids, and solubilized more than half of the lignin, representing the optimal compromise between sugar preservation and oil yield. In addition, analysis of the hexane-extracted fraction revealed a mixture of lipid-derived esters (*e.g.*, fatty acid methyl esters, monoglycerides, diglycerides, and triglycerides) and lignin monomers/dimers; these species are compatible with hydrotreating and hydrodeoxygenation and can be upgraded toward jet-range alkanes and aromatics. Analysis of lignin-rich oil revealed a broad distribution of phenolics, with approximately 48–51% of its mass falling within the 110–450 Da range, indicating that a significant portion of this oil could be upgraded to SAF blendstocks *via* hydrodeoxygenation (HDO). Overall, methanol-driven solvolysis recovered ~66% of the total SCG mass as viable feedstock for downstream SAF pathways (Fig. 6). This recovery includes fermentable sugars in a carbohydrate-rich solid residue suitable for ethanol-to-jet conversion, a hexane-extracted oil fraction containing lipid-derived esters and lignin monomers/dimers for hydrotreating, and a SAF-convertible fraction of lignin-rich oil in the monomer–dimer range for HDO.

The resulting minimum selling price (MSP) of the oil (\$2.05 per kg), the combined hexane-extracted oil and SAF-range fraction of the undissolved lignin-rich oil, remains competitive when benchmarked against commercial SAF feedstock costs: recent U.S. Department of Agriculture forecasts place soybean

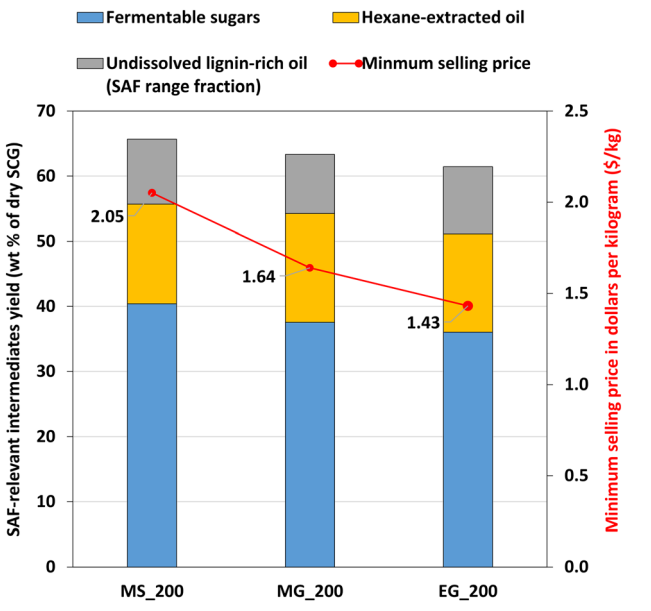

Fig. 6 SAF-intermediate product yields (fermentable sugars and SAF-intermediate oil products) and corresponding minimum selling prices (MSP; \$ per kg) for methanol (MS_200), methanol/glycerol (MG_200), and ethanol/glycerol (EG_200) solvolysis at 200 °C.

oil (dominant HEFA feedstock) at roughly $1.17 per kg, while the National Renewable Energy Laboratory's HEFA pathway analysis shows that feedstock price fluctuations can drive minimum fuel selling prices anywhere from $0.60 to $3.10 per kg, underscoring the sensitivity of SAF costs to feedstock markets.[13] This comparison suggests that the SCG-derived MSP is within the same order of magnitude as current SAF feedstock costs, particularly when considering price volatility. However, methanol-based solvolysis generated the highest autogenous pressure (38.0 bar), raising both safety concerns and equipment costs.

Substituting methanol with co-solvent systems of methanol/glycerol (MG) or ethanol/glycerol (EG) significantly reduced operating pressure while maintaining comparable fractionation performance. MG lowered the pressure to 19.1 bar, while EG achieved 15.6 bar, a 59% reduction relative to methanol, without substantial losses in fractionation efficiency and resulting SAF-intermediate oil yield (Fig. 6). EG further delivered the lowest MSP ($1.43 per kg), benefiting from reduced capital expenditure, safer operation, and complete solvent circularity, as ethanol can be sourced from sugar fermentation and glycerol from lipid transesterification. This co-solvent strategy aligns with circular economy principles, enabling solvent self-sufficiency, reducing process severity, and improving scalability. Taken together, this work advances beyond oil/extractive-focused SCG processing by implementing an integrated whole-biomass solvolysis and separation framework that quantitatively resolves all major SCG fractions into distinct streams with high mass closure. Coupled with stream-resolved characterization and TEA, the study demonstrates how solvent configuration and endogenous solvent circulation influence system-level process performance for SAF-intermediate production.

Despite the promising results of endogenous solvent-driven valorization of SCG to SAF, several technical challenges must be addressed for scale-up. Current alcohol-based solvolysis requires dry biomass feedstock to minimize carbohydrate solubilization, necessitating energy-intensive drying operations that undermine process economics. Future efforts should explore partial moisture tolerance or incorporate water as a co-solvent under controlled conditions, despite its tendency to leach sugars. Glycerol separation presents another challenge, as water extraction dissolves significant lignin because glycerol acts as a co-solvent that enhances lignin solubility in the aqueous phase. This complicates product recovery and increases downstream purification requirements. Alternative separation strategies, such as membrane filtration or distillation, may offer more efficient glycerol removal while preserving lignin-rich oil yields.

Product upgrading also poses difficulties, as the hexane-extracted oil contains both alkyl esters and lignin-derived phenolics. This heterogeneous mixture requires multifunctional catalysts capable of co-processing lipid- and lignin-derived intermediates into SAF-range hydrocarbons. Likewise, upgrading of carbohydrate-rich solid residues and further conversion of lignin-derived fractions to defined SAF-range cuts must be experimentally demonstrated to confirm the feasibility of an integrated SCG-to-SAF pathway. Finally, feedstock variability from differences in bean type, roasting, and brewing methods affects fractionation efficiency, product yields, and solvent balance. The feedstock flexibility of this approach remains to be demonstrated, with future work needed to identify reaction conditions and solvent systems that minimize performance variability across diverse SCG sources.

Author contributions

CA: conceptualization, analysis, writing, investigation, review and editing. KCJ, VTW, VGN: analysis, investigation, review and editing. EA, WBB, IES, JEK: analysis, review and editing. JFS: writing, review and editing. JHJ: conceptualization, investigation, supervision, funding acquisition, writing, review and editing.

Conflicts of interest

The authors declare no conflicts of interest.

Data availability

The data that support the findings of this study are available in the supplementary information (SI). The SI contains detailed experimental procedures, analytical and calibration methods, compositional analysis, NMR, FT-IR and GPC analyses, and techno-economic analysis assumptions and cost breakdowns. Supplementary information is available. See DOI: https://doi.org/10.1039/d5gc06813d.

Acknowledgements

The authors thank Matthew J. Toht for assisting with experiments for the compositional analysis. We extend our thanks to Jessica Rudolph and Justin Elko of the Advanced Materials and Manufacturing Institute, and Rob McClernan and Larissa Huber of the Department of Chemical Engineering at Rowan University for their assistance with the project. This work was supported by the Sustainable Futures Initiative Grant Program: Early Career Postdoctoral-Faculty Bridge Grant, grant no. 67859-ECP of the ACS Campaign for a Sustainable Future. JHJ served as Principal Investigator on Grant 67859-ECP that provided support for WBB. The USDA-ARS supported this work under project number 8072-41000-111.

Mention of trade names or commercial products in this publication is solely for providing specific information and does not imply recommendation or endorsement by the U.S. Department of Agriculture. USDA is an equal opportunity provider and employer.

References

1 U.S. Department of Transportation, 2024 *United States Aviation Climate Action Plan*, https://www.epa.gov/system/files/documents/2024-12/us-aviation-state-action-plan-2024-final.pdf.

2 IEA Bioenergy, *Progress in Commercialization of Biojet/Sustainable Aviation Fuels (SAF): Technologies and Policies*, https://www.ieabioenergy.com/wp-content/uploads/2024/06/IEA-Bioenergy-Task-39-SAF-report.pdf.

3 U.S. Department of Energy (DOE), U.S. Department of Transportation (DOT) and U.S. Department of Agriculture (USDA), *Sustainable Aviation Fuel Grand Challenge Roadmap: Flight Plan for Sustainable Aviation Fuel*, https://www.energy.gov/sites/default/files/2022-09/beto-saf-gc-roadmap-report-sept-2022.pdf.

4 The White House, Fact Sheet: Biden Administration Advances the Future of Sustainable Fuels in American Aviation, https://bidenwhitehouse.archives.gov/briefing-room/statements-releases/2021/09/09/fact-sheet-biden-administration-advances-the-future-of-sustainable-fuels-in-american-aviation/.

5 U.S. Department of Agriculture (USDA), USDA Joins Government-Wide Sustainable Aviation Fuels Grand Challenge, https://www.usda.gov/about-usda/news/press-releases/2021/09/09/usda-joins-government-wide-sustainable-aviation-fuels-grand-challenge.

6 European Union Aviation Safety Agency (EASA), EASA releases status report on Europe's SAF production and preparedness, https://www.greenairnews.com/?p=6447.

7 International Civil Aviation Organization (ICAO), *ICAO Environmental Report* 2019 – Chapter 6*: CORSIA*, https://www2023.icao.int/environmental-protection/CORSIA/Documents/ICAO%20Environmental%20Report%202019_Chapter%206.pdf.

8 International Airport Review, IATA Reveals SAF Production Growth in 2024, Urges Acceleration to Meet Decarbonisation Targets, https://www.internationalairportreview.com/news/232770/iata-reveals-saf-production-growth-in-2024-urges-acceleration-to-meet-decarbonisation-targets/.

9 KnowESG, SAF Production Increased but Fell Short of 2024 Projections, https://www.knowesg.com/environment/saf-production-increased-but-fell-short-of-2024-projections-11122024.

10 M. S. Webber, J. Watson, J. Zhu, J. H. Jang, M. Caglayan, J. S. Heyne, G. T. Beckham and Y. Roman-Leshkov, *Nat. Mater.*, 2024, **23**, 1622–1638.

11 C. Gutiérrez-Antonio, F. I. Gómez-Castro, J. A. de Lira-Flores and S. Hernández, *Renewable Sustainable Energy Rev.*, 2017, **79**, 709–729.

12 M. Song, X. Zhang, Y. Chen, Q. Zhang, L. Chen, J. Liu and L. Ma, *Energy*, 2023, **283**, 129107.

13 National Renewable Energy Laboratory (NREL), *Sustainable Aviation Fuel State-of-Industry Report: Hydroprocessed Esters and Fatty Acids (HEFA)*, https://www.nrel.gov/docs/fy24osti/87803.pdf.

14 SkyNRG, The Basics of SAF Technology | The HEFA Process, https://skynrg.com/sustainable-aviation-fuel/technology-basics/.

15 World Energy, Sustainable Aviation Fuel Production at World Energy, https://worldenergy.net/our-approach/book-claim/.

16 Valero, *ESG Report*, https://www.paperturn-view.com/valero/2024-esg-report-final?pid=ODg8828383&p=79&v=3.1.

17 S. Xie, Z. Li, S. Luo and W. Zhang, *Renewable Sustainable Energy Rev.*, 2024, **192**, 114240.

18 P. Dhungana, B. Prajapati, S. Maharjan and J. Joshi, *Int. J. Appl. Sci. Biotechnol.*, 2022, **10**, 1–11.

19 M. M. Uddin, U. Lee, H. Xu, Y. Li, H. Kwon, Y. Zhang, S. Smolinski, H. Cai and L. Tao, *Appl. Energy*, 2025, **398**, 304–317.

20 U.S. Department of Energy, *Sustainable Aviation Fuel: Review of Technical Pathways*, https://www.energy.gov/sites/prod/files/2020/09/f78/beto-sust-aviation-fuel-sep-2020.pdf.

21 M. S. Webber, Z. Yang, D. C. Bell, D. G. Brandner, J. R. Bussard, J. Watson, M. L. Stone, X. Wu, Q. S. Neuendorf, L. C. Myers, J. S. Heyne, G. T. Beckham and Y. Román-Leshkov, *Cell Rep. Phys. Sci.*, 2025, **6**, 102687.

22 M. L. Stone, M. S. Webber, W. P. Mounfield, D. C. Bell, E. Christensen, A. R. C. Morais, Y. Li, E. M. Anderson, J. S. Heyne, G. T. Beckham and Y. Román-Leshkov, *Joule*, 2022, **6**, 2324–2337.

23 National Renewable Energy Laboratory (NREL), *Sustainable Aviation Fuel (SAF) State-of-Industry Report: State of SAF Production Process*, NREL/TP-5100-87802, 2024, https://docs.nlr.gov/docs/fy24osti/87802.pdf.

24 McKinsey & Company, Global Energy Perspective 2023: Sustainable Fuels Outlook, https://www.mckinsey.com/industries/oil-and-gas/our-insights/global-energy-perspective-2023-sustainable-fuels-outlook.

25 KPMG UK, Sustainable Aviation Fuel, https://kpmg.com/uk/en/insights/sustainability/sustainable-aviation-fuel.html.

26 Sustainable Aviation Fuel Market Outlook, The State of the SAF Market in 2022 and Beyond, https://flysaba.org/2022/12/15/state-of-saf-market-2022-and-beyond/.

27 International Council on Clean Transportation (ICCT), Estimating Sustainable Aviation Fuel Feedstock Availability to Meet Climate Goals, https://theicct.org/wp-content/uploads/2021/06/Sustainable-aviation-fuel-feedstock-eu-mar2021.pdf.

28 International Renewable Energy Agency (IRENA), *Reaching Zero with Renewables: Biojet Fuels*, https://www.irena.org/-/media/Files/IRENA/Agency/Publication/2021/Jul/IRENA_Reaching_Zero_Biojet_Fuels_2021.pdf.

29 RMI, *Refueling Aviation in the United States*, https://rmi.org/wp-content/uploads/dlm_uploads/2024/02/refueling_aviation_in_united_states_report.pdf.

30 T. A. Kurniawan, *BioResources*, 2025, **20**, 4821–4860.

31 C. M. Mendieta, J. Kruyeniski, M. E. Vallejos and M. C. Area, *BioResources*, 2024, **20**, 11–14.

32 F. H. Isikgor and C. R. Becer, *Polym. Chem.*, 2015, **6**, 4497–4559.

33 Y. Zhao, K. Lu, H. Xu, L. Zhu and S. Wang, *Renewable Sustainable Energy Rev.*, 2021, **139**, 110706.
34 J. M. Perez, W. S. Kontur, M. Alherech, J. Coplien, S. D. Karlen, S. S. Stahl, T. J. Donohue and D. R. Noguera, *Green Chem.*, 2019, **21**, 1340–1350.
35 M. Madadi, M. Saleknezhad, S. S. Hashemi, E. Kargaran, M. Abbasi-Riyakhuni, D. Cai, A. Priyadarshini, M. Elsayed, C. Sun and F. Sun, *Biofuel Res. J.*, 2025, **12**, 2554–2568.
36 M. Madadi, E. Kargaran, S. S. Hashemi, C. Sun, J. F. M. Denayer, K. Karimi, F. Sun and V. K. Gupta, *Adv. Sci.*, 2025, **12**, e10496.
37 G. Song, P. Teng, M. Madadi, H. Hadiyanto, C. Sun, J. Hu and F. Sun, *Carbohydr. Polym.*, 2025, **370**, 124363.
38 M. J. Gan, Y. Q. Niu, X. J. Qu and C. H. Zhou, *Green Chem.*, 2022, **24**, 7705–7750.
39 Y. Li, S. S. Bhagwat, Y. R. Cortés-Peña, D. Ki, C. V. Rao, Y.-S. Jin and J. S. Guest, *ACS Sustainable Chem. Eng.*, 2021, **9**, 1341–1351.
40 P. E. Marriott, L. D. Gomez and S. J. McQueen-Mason, *New Phytol.*, 2016, **209**, 1366–1381.
41 N. Kondamudi, S. K. Mohapatra and M. Misra, *J. Agric. Food Chem.*, 2008, **56**, 11757–11760.
42 F. Battista, E. M. Barampouti, S. Mai, D. Bolzonella, D. Malamis, K. Moustakas and M. Loizidou, *Renewable Sustainable Energy Rev.*, 2020, **131**, 110007.
43 R. Campos-Vega, G. Loarca-Piña, H. A. Vergara-Castañeda and B. D. Oomah, *Trends Food Sci. Technol.*, 2015, **45**, 24–36.
44 B. Yusufoğlu, G. Kezer, Y. Wang, Z. M. Ziora and T. Esatbeyoglu, *Curr. Opin. Food Sci.*, 2024, **55**, 101111.
45 A. B. Ozturk, N. Jakovljevic, G. Semaan and G. Kumar, *Biomass Bioenergy*, 2025, **202**, 108220.
46 W.-T. Tsai, S.-C. Liu and C.-H. Hsieh, *J. Anal. Appl. Pyrolysis*, 2012, **93**, 63–67.
47 J. Simoes, F. M. Nunes, M. R. Domingues and M. A. Coimbra, *Carbohydr. Polym.*, 2013, **97**, 81–89.
48 K. Johnson, Y. Liu and M. Lu, *Front. Chem. Eng.*, 2022, **4**, 838605.
49 E. Bevilacqua, V. Cruzat, I. Singh, R. B. Rose'Meyer, S. K. Panchal and L. Brown, *Nutrients*, 2023, **15**, 994.
50 K. P. Krakowiak, R. D. McIntosh and D. Ellis, *Sustainable Food Technol.*, 2024, **2**, 92–103.
51 M. Lauberts, I. Mierina, M. Pals, M. A. A. Latheef and A. Shishkin, *Plants*, 2022, **12**, 30.
52 I. Efthymiopoulos, P. Hellier, N. Ladommatos, A. Kay and B. Mills-Lamptey, *Waste Biomass Valorization*, 2019, **10**, 253–264.
53 R. Ravindran, S. Jaiswal, N. Abu-Ghannam and A. K. Jaiswal, *Bioresour. Technol.*, 2017, **239**, 276–284.
54 T. Jooste, M. P. Garcia-Aparicio, M. Brienzo, W. H. van Zyl and J. F. Gorgens, *Appl. Biochem. Biotechnol.*, 2013, **169**, 2248–2262.
55 E. E. Kwon, H. Yi and Y. J. Jeon, *Bioresour. Technol.*, 2013, **136**, 475–480.
56 L. Jenicek, B. Tunklova, J. Malatak, M. Neskudla and J. Velebil, *Materials*, 2022, **15**, 6722.
57 M. M. Tun, H. Raclavska, D. Juchelkova, J. Ruzickova, M. Safar, K. Strbova and P. Gikas, *J. Environ. Manage.*, 2020, **275**, 111204.
58 H. V. Ly, B. Lee, J. W. Sim, Q. K. Tran, S.-S. Kim, J. Kim, B. Brigljević, H. T. Hwang and H. Lim, *Chem. Eng. J.*, 2022, **427**, 130956.
59 J. B. Tarigan, M. Ginting, S. N. Mubarokah, F. Sebayang, J. Karo-Karo, T. T. Nguyen, J. Ginting and E. K. Sitepu, *RSC Adv.*, 2019, **9**, 35109–35116.
60 I. Chiyanzy, M. Brienzo, M. García-Aparicio, R. Agudelo and J. Görgens, *J. Chem. Technol. Biotechnol.*, 2014, **90**, 449–458.
61 J. Pereira, M. M. R. de Melo, C. M. Silva, P. C. Lemos and L. S. Serafim, *Bioengineering*, 2022, **9**, 362.
62 J. Huang, B. Li, X. Xian, Y. Hu and X. Lin, *Fermentation*, 2024, **10**, 362.
63 T. Renders, S. Van den Bosch, S. F. Koelewijn, W. Schutyser and B. F. Sels, *Energy Environ. Sci.*, 2017, **10**, 1551–1557.
64 E. M. Anderson, M. L. Stone, R. Katahira, M. Reed, G. T. Beckham and Y. Román-Leshkov, *Joule*, 2017, **1**, 613–622.
65 I. Kumaniaev, E. Subbotina, J. Sävmarker, M. Larhed, M. V. Galkin and J. S. M. Samec, *Green Chem.*, 2017, **19**, 5767–5771.
66 M. Oliet, J. García, F. Rodríguez and M. A. Gilarrranz, *Chem. Eng. J.*, 2002, **87**, 157–162.
67 G. Tofani, E. Jasiukaitytė-Grojzdek, M. Grilc and B. Likozar, *Green Chem.*, 2024, **26**, 186–201.
68 J. Son, B. Kim, J. Park, J. Yang and J. W. Lee, *Bioresour. Technol.*, 2018, **259**, 465–468.
69 M. M. Abu-Omar, K. Barta, G. T. Beckham, J. S. Luterbacher, J. Ralph, R. Rinaldi, Y. Román-Leshkov, J. S. M. Samec, B. F. Sels and F. Wang, *Energy Environ. Sci.*, 2021, **14**, 262–292.
70 R. G. Bitencourt, F. M. P. A. Mello, F. A. Cabral and A. J. A. Meirelles, *J. Supercrit. Fluids*, 2020, **157**, 104689.
71 M. N. Araujo, K. C. dos Santos, N. do Carmo Diniz, J. C. de Carvalho and M. L. Corazza, *Bioresour. Technol. Rep.*, 2022, **18**, 101013.
72 F. Battista, L. Zuliani, F. Rizzioli, S. Fusco and D. Bolzonella, *Bioresour. Technol.*, 2021, **342**, 125952.
73 I. Corrado, R. Argenziano, E. Borselleca, F. Moccia, L. Panzella and C. Pezzella, *Sep. Purif. Technol.*, 2024, **334**, 125998.
74 F. Sun and H. Chen, *Bioresour. Technol.*, 2008, **99**, 5474–5479.
75 F. F. Sun, L. Wang, J. Hong, J. Ren, F. Du, J. Hu, Z. Zhang and B. Zhou, *Bioresour. Technol.*, 2015, **187**, 354–361.
76 D. S. Zijlstra, C. W. Lahive, C. A. Analbers, M. B. Figueirêdo, Z. Wang, C. S. Lancefield and P. J. Deuss, *ACS Sustainable Chem. Eng.*, 2020, **8**, 5119–5131.
77 K. Tekin, N. Hao, S. Karagoz and A. J. Ragauskas, *ChemSusChem*, 2018, **11**, 3559–3575.
78 F. Ma and M. A. Hanna, *Bioresour. Technol.*, 1999, **70**, 1–15.
79 Y. Sun and J. Cheng, *Bioresour. Technol.*, 2002, **83**, 1–11.
80 C. Sun, H. Ren, F. Sun, Y. Hu, Q. Liu, G. Song, A. Abdulkhani and P. L. Show, *Bioresour. Technol.*, 2022, **344**, 126264.

81 X. Pan, C. Arato, N. Gilkes, D. Gregg, W. Mabee, K. Pye, Z. Xiao, X. Zhang and J. Saddler, *Biotechnol. Bioeng.*, 2005, **90**, 473–481.
82 B. B. Hallac, Y. Pu and A. J. Ragauskas, *Energy Fuels*, 2010, **24**, 2723–2732.
83 C. Chotirotsukon, M. Raita, V. Champreda and N. Laosiripojana, *Ind. Crops Prod.*, 2019, **141**, 111753.
84 P. P. Thoresen, L. Matsakas, U. Rova and P. Christakopoulos, *Bioresour. Technol.*, 2020, **306**, 123189.
85 G. Song, M. Madadi, X. Meng, C. Sun, M. Aghbashlo, F. Sun, A. J. Ragauskas, M. Tabatabaei and A. Ashori, *Chem. Eng. J.*, 2024, **481**, 148713.
86 G. G. Facas, D. G. Brandner, J. R. Bussard, Y. Román-Leshkov and G. T. Beckham, *ACS Sustainable Chem. Eng.*, 2023, **11**, 4517–4522.
87 D. Dolan, R. Brucato, C. Reid, A. F. Lee, K. Wilson and A. M. Voutchkova-Kostal, *Chem. Sci.*, 2024, **15**, 20223–20239.
88 National Renewable Energy Laboratory (NREL), *Determination of Structural Carbohydrates and Lignin in Biomass: Laboratory Analytical Procedure (LAP)*, https://docs.nrel.gov/docs/gen/fy13/42618.pdf.
89 F. Calixto, J. Fernandes, R. Couto, E. J. Hernández, V. Najdanovic-Visak and P. C. Simões, *Green Chem.*, 2011, **13**, 1196–1202.
90 J. Park, B. Kim and J. W. Lee, *Bioresour. Technol.*, 2016, **221**, 55–60.
91 S. Van den Bosch, W. Schutyser, R. Vanholme, T. Driessen, S. F. Koelewijn, T. Renders, B. De Meester, W. J. J. Huijgen, W. Dehaen, C. M. Courtin, B. Lagrain, W. Boerjan and B. F. Sels, *Energy Environ. Sci.*, 2015, **8**, 1748–1763.
92 J. H. Jang, D. G. Brandner, R. J. Dreiling, A. J. Ringsby, J. R. Bussard, L. M. Stanley, R. M. Happs, A. S. Kovvali, J. I. Cutler, T. Renders, J. R. Bielenberg, Y. Román-Leshkov and G. T. Beckham, *Joule*, 2022, **6**, 1859–1875.
93 Y. Liu, W. Chen, Q. Xia, B. Guo, Q. Wang, S. Liu, Y. Liu, J. Li and H. Yu, *ChemSusChem*, 2017, **10**, 1692–1700.
94 R. K. Saini, P. Prasad, X. Shang and Y. S. Keum, *Int. J. Mol. Sci.*, 2021, **22**, 13643.